Integration of reservoir simulation with time-lapse seismic modelling

Ying Zou, Laurence R. Bentley, and Laurence R. Lines

ABSTRACT

Time-lapse seismic modelling was conducted for the Pikes Peak heavy oilfield using the results from a reservoir simulation model. Cyclical steam stimulation (CSS) started in 1981 and continues to the present. A flow simulation model was constructed for the region around a seismic profile that was conducted in 1991 and repeated in 2000. The simulator was run from the start of production in 1981 through 2000. The porosity, saturation, pressure, and temperature were extracted from the reservoir zone from the flow simulator for the pre-production condition and at the times of the 1991 and 2000 surveys. The seismic response of the reservoir was computed using a fluid substitution procedure and forward modelling. Comparing the results of these three times indicated that the gas saturation changes caused the largest change in the simulated seismic response. Seismic difference sections showed that thick zones of gas saturation caused changes in reflection from the tops and bottoms of the reservoir as well as differences deeper in the section due to time delays caused by lower velocity within the reservoir zone. Thin zones of gas caused reflection amplitude differences, but not time delay differences. Temperature and pressure were also correlated with seismic changes, but not as strongly as the gas saturation. However, the changes in the moduli with effective stress changes have not yet been incorporated in the rock physics model. In the future, the simulated seismic response changes will be compared to the measured seismic response changes, and the reservoir simulation parameters will be adjusted to match both the production history and the seismic history.

INTRODUCTION

Knowledge of the spatial variation of reservoir parameters such as porosity, pore-fluid content, permeability, pressure, and temperature are critical to accurately evaluate the total volume of recoverable hydrocarbon reserves in place and to predict fluid flow in the reservoir. Reservoir simulation is often used to help understand the changes in reservoir conditions with the stages of production. Reservoir simulation is based on models that are created from well information, seismic data and geologic maps. The results around wells are controlled by engineering data, but the results between or beyond wells cannot be verified by engineering data. Seismic surveys can be used to interpolate or extrapolate reservoir information between or beyond wells. Through rock physics equations, seismic properties such as velocity and density can be estimated from the output of reservoir simulation for seismic modelling. Synthetic seismic sections can be created and compared with the sections of field seismic surveys. By analyzing the differences between the synthetic seismic section based on the reservoir simulation and the real seismic sections, we can update the reservoir model and locate the remaining oil and trace steam fronts. There is a recognized need to combine the skills of geoscientists and engineers to build optimized reservoir models that incorporate all available engineering, geological and geophysical data. There are some early research works that construct seismic models using reservoir simulation output (Lumley, 1995) for primary depletion.

There are also some published seismic modelling works and simplified reservoir simulation works on steam-based recovery reservoirs (Jenkins, Waite, and Bee, 1997; Eastwood et al., 1994).

To effectively integrate reservoir simulation with seismic modelling, we employed a detailed reservoir model and real production history data. This work focuses on the conversion of reservoir simulations to seismic sections for the Pikes Peak heavy oilfield and it is a part of an ongoing combined study of seismic survey analysis, reservoir simulation and seismic modelling. With PVT data, permeability, porosity and production history data from Husky, we undertook history matching for the partial reservoir that encompasses 140 metres on either side of two time-lapse seismic lines in the Pikes Peak heavy oilfield. We previously designed a procedure (Zou and Bentley, 2003) to calculate velocity and density from the reservoir saturations, temperature, pressure, and porosity distributions resulted derived from reservoir simulations based on several empirical relations (Batzle and Wang, 1992). For different producing stages, synthetic seismic sections were created. The simulated reservoir changes after 10 years of production cause significant changes in the synthetic seismic sections.

GEOLOGY, GEOPHYSICAL AND ENGINEERING BACKGROUND

Pikes Peak oilfield is located on the border of Alberta and Saskatchewan. The producing reservoir is in the Lower Cretaceous Waseca Formation. It is about 500 metres below the surface. The reservoir's porosity is around 0.32~0.36 and with 80% heavy oil saturation. The Waseca Formation production zone has been divided into a homogeneous, well-sorted, predominantly quartz lower unit, and a sand-shale interbedded upper unit (Sheppard, Wong, and Love, 1998; Miller and Given, 1989). Steam-drive technology has been applied to enhance recovery by reducing the effective viscosity of the oil. Husky Oil acquired a set of 2D swath lines in the north-south direction in 1991. To investigate time-lapse effects, the University of Calgary and Husky acquired a repeat line on the eastern side of the field in 2000. A successful Cyclic Steam Stimulation (CSS) started at Pikes Peak in 1981. In the eastern part of the reservoir, CSS has been in operation since 1983. Table 1 contains the basic reservoir properties and Figure 1 shows typical logs from well 1A15 (X6i in Figure 2).

Table 1. Pikes Peak Waseca Channel homogeneous unit reservoir properties

Depth	500 m
Initial temperature	18 ^{o}C
Initial pressure	3350 KPa
Net pay (including lower interbed)	5.7 – 27.5 m
Air permeability	4500-10,000 md
Porosity	0.32 – 0.36
Water saturation	0.08 – 0.22
Oil density	985kg/m^3
Dead oil viscosity	25,000 mPa.s
Oil formation volume factor	1.025 m^3/m^3
Initial GOR	14.5 m^3/m^3
Oil Saturation	0.80 – 0.90

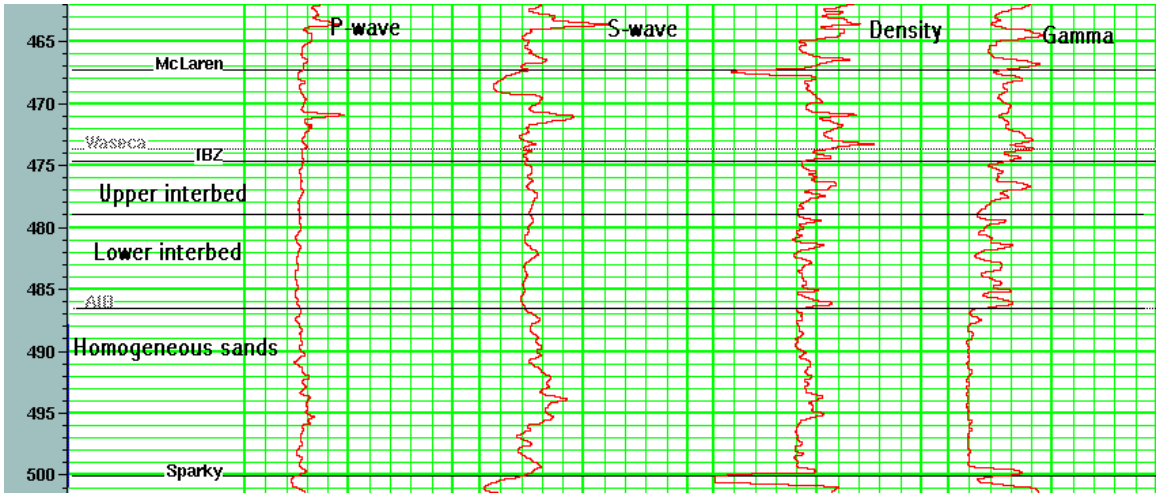

FIG. 1. P-wave, S-wave, density, and gamma logs from well 1A15.

RESERVOIR SIMULATION AND RESULTS

The reservoir model for the present reservoir simulation was built by Husky Oil. The reservoir grid geometry, well locations, and time-lapse seismic line location are shown in Figure 2. The seismic lines are in the middle of the reservoir in north-south direction. The 1991 and 2000 surveys are separated by 5 m. The grid dimension is 20 by 20m. There are three vertical layers with varying thickness.

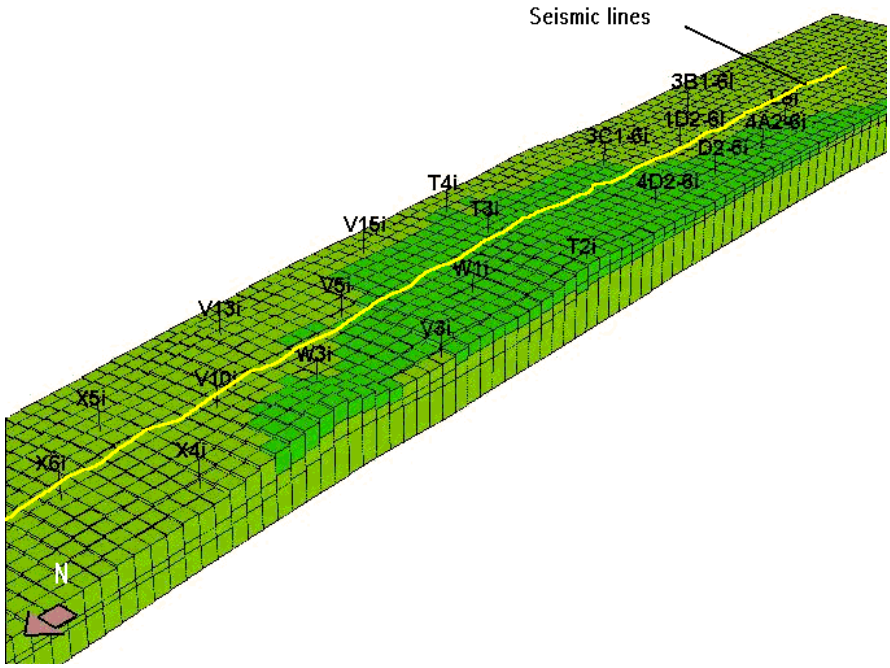

FIG. 2. Reservoir geometry and time-lapse seismic line location.

To date we have considered the three layers as having individually uniform but distinctive properties. A single simulation takes 24 hours.

CSS started in the southern part of the reservoir in 1983 at well 1D2-6. Average steam injection duration was 10 to 30 days followed by 5 to 10 months of soak and production. The reservoir simulation is based on the injection and production history from Jan. 1981 to Aug. 2003. Preliminary history matching results for two wells are shown in Figure 3 and 4. Other wells close to the seismic lines have similar results. For well 1D2-6, the cumulative liquid production from simulation is somewhat lower than the history data. The simulated bottom hole pressure (BHP), dropped rapidly in early 1985. When

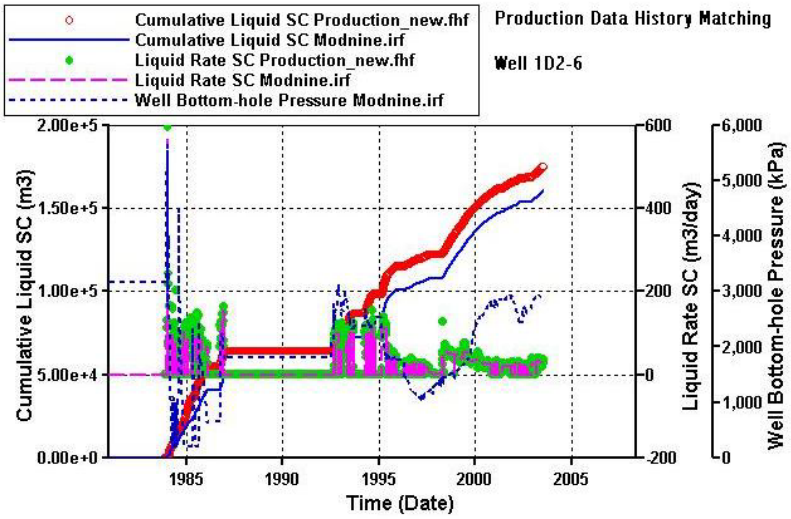

FIG. 3. History matching results for liquid rate, cumulative liquid, and bottom hole pressure for well 1D2-6. The red dots are the cumulative liquid productions in standard condition from the history file. The blue solid line is the cumulative liquid production in standard condition from the simulation output. The green dots are the liquid rate in standard condition from the history file. The pink dash line is the liquid rate in standard condition from the simulation output. The blue dash line is the well bottom-hole pressure from the simulation output.

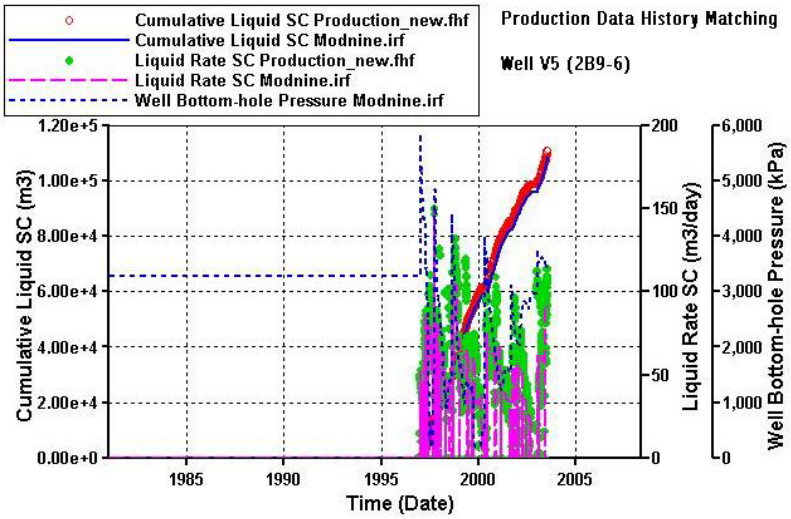

FIG. 4. History matching results for liquid rate, cumulative liquid, and bottom hole pressure for well V5. The red dots are the cumulative liquid productions in standard condition from the history file. The blue solid line is the cumulative liquid production in standard condition from the simulation output. The green dots are the liquid rate in standard condition from the history file. The pink dash line is the liquid rate in standard condition from the simulation output. The blue dash line is the well bottom-hole pressure from the simulation output.

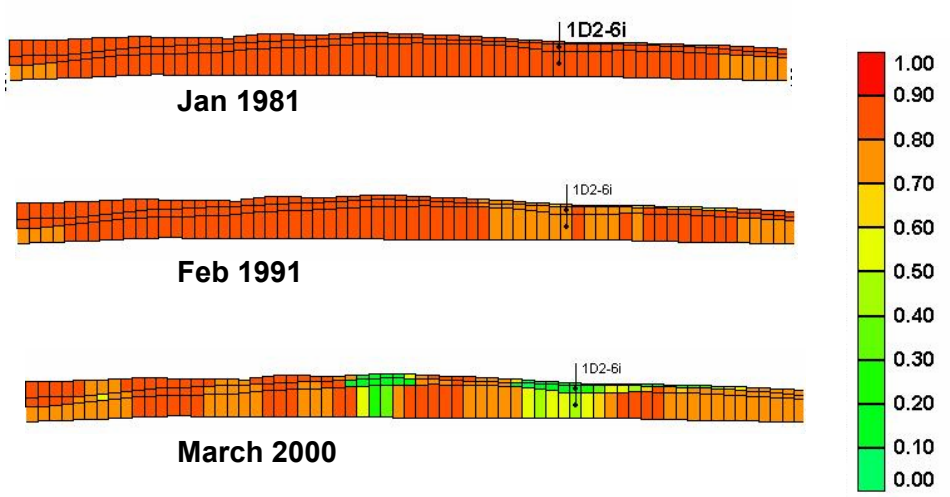

FIG. 5. Oil saturations from reservoir simulation at three dates.

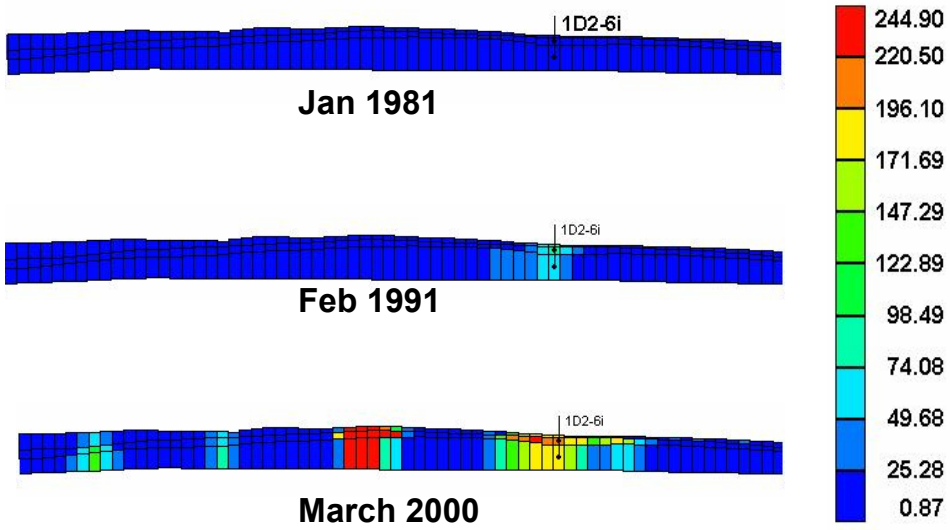

FIG. 6. Temperature (^{o}C) from reservoir simulation at three dates.

BHP reached the producer pressure constraint of 202Kpa, the simulated production stopped causing the average production rate to be too low. This is also the case for well 2B9-6 although the production history mismatch is not as large as for well 1D2-6. The liquid production rates applied in the data file were the same as the history data. The well 2B9-6 mismatch might be due to numerical problems related to the well index or pressure constraint or pressure support from outside the model boundaries. Work remains to fine-tune the history match. Figures 5 and 6 show the oil saturation and temperature respectively on the profile where seismic lines are located. The high temperature area

corresponds to the area in which the oil saturation has decreased. Figures 7 and 8 show reservoir pressure and gas saturation along the profile, respectively. Reservoir pressure mainly depends on whether the simulation is in injection stage or production stage. The pressure seems to affect the gas saturation. The pressure front spreads much faster than the temperature. The gas saturation here is for a gas phase and is constituted of different components such as water vapour and methane.

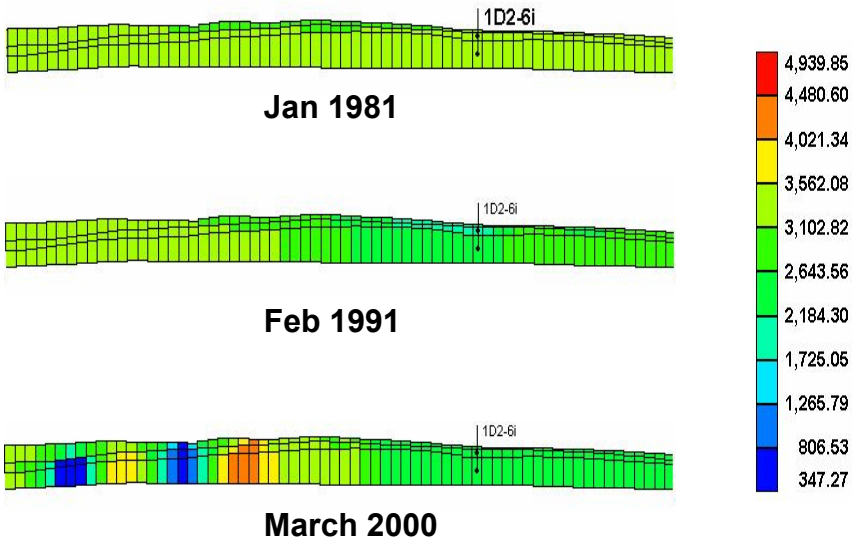

FIG. 7. Pressure (KPa) from reservoir simulation at three dates.

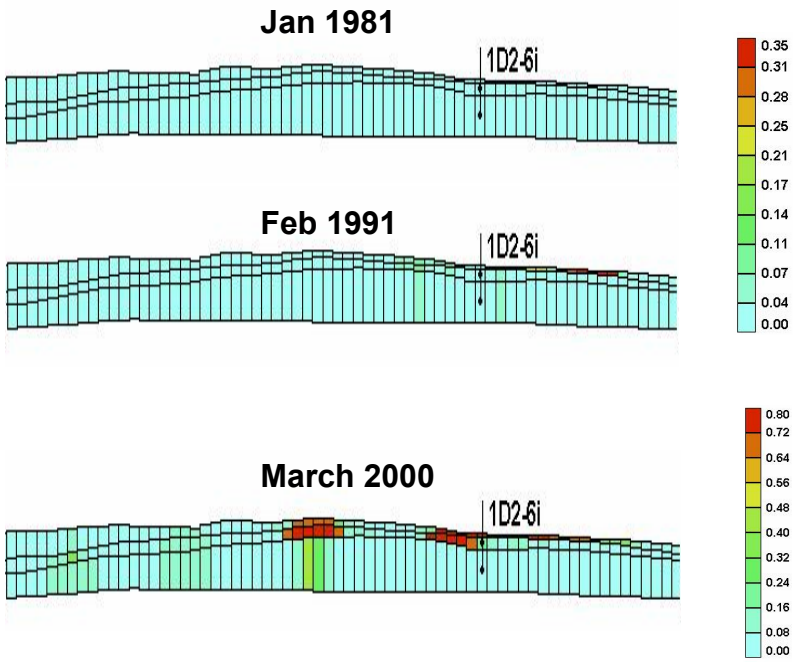

FIG. 8. Gas saturation from reservoir simulation at three dates.

Figure 9 shows 3D temperature snap shots in Jan 1981, Feb 1991 and March 2000. Temperature increase represents steam progress. The steam front moves about 5 m to 8 m per year. It spreads faster in the north-south direction than in the east-west direction.

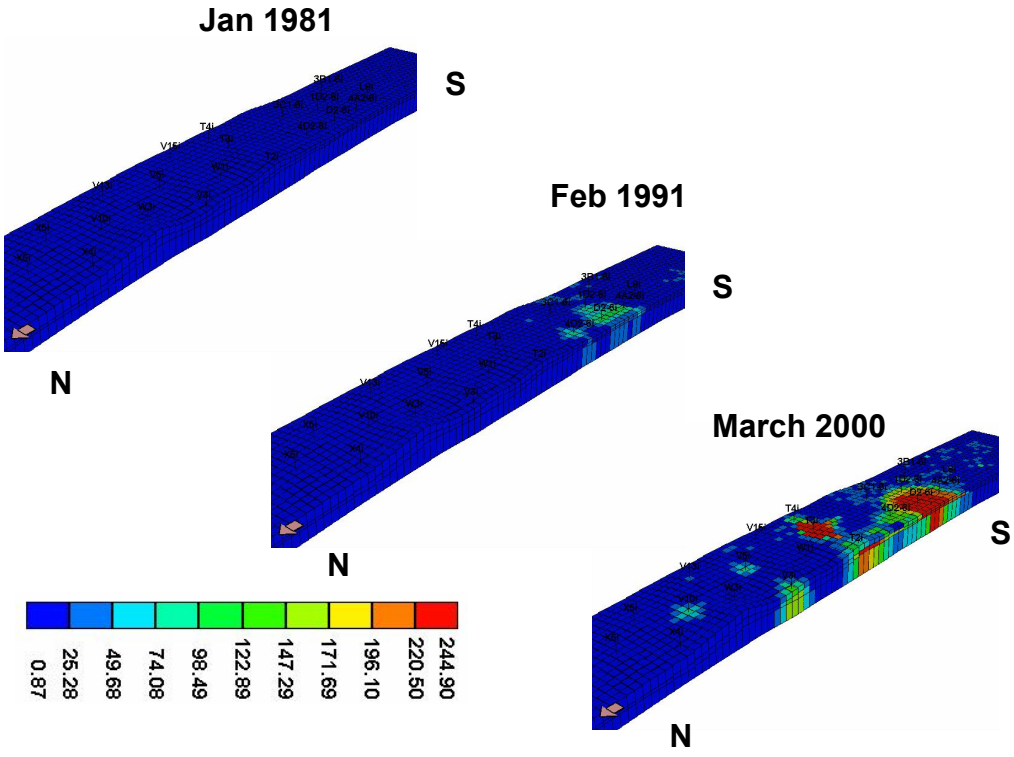

FIG. 9. Temperature (^{o}C) from reservoir simulation.

SYNTHETIC SEISMIC SECTIONS

Based on a previously described rock physics procedure (Zou and Bentley, 2003), we used the reservoir simulation output to calculate velocity and density for the 2D profile where the seismic lines were located. Since the time-lapse seismic surveys were in Feb. 1991 and March 2000, we did these calculations for these two time steps plus initial pre-production time, Jan 1981. Using the procedure described in previous seismic modelling work (Zou, Bentley and Lines, 2003), we constructed velocity and density model using well logs for regions outside of the reservoir and calculated velocity and density using reservoir simulation output for the regions within the reservoir. After the model was built, we generated a zero-offset synthetic seismic section using a Gaussian wavelet with a central frequency of 60 Hz. These sections were then migrated. Usually the reservoir simulation mesh is different than the seismic grid, and the simulation mesh needs to be revised to make it compatible with the seismic modelling. For this case, the reservoir grid elements are 20 m by 20 m and the grid thickness varies from 1 m to 10 m. To make the model the same as the real seismic section in which the CDP interval is 10 m, we interpolated one trace between every two grids nodes. The velocity and density models were sub-sampled to 2 metres to make the models smooth across the reservoir boundaries.

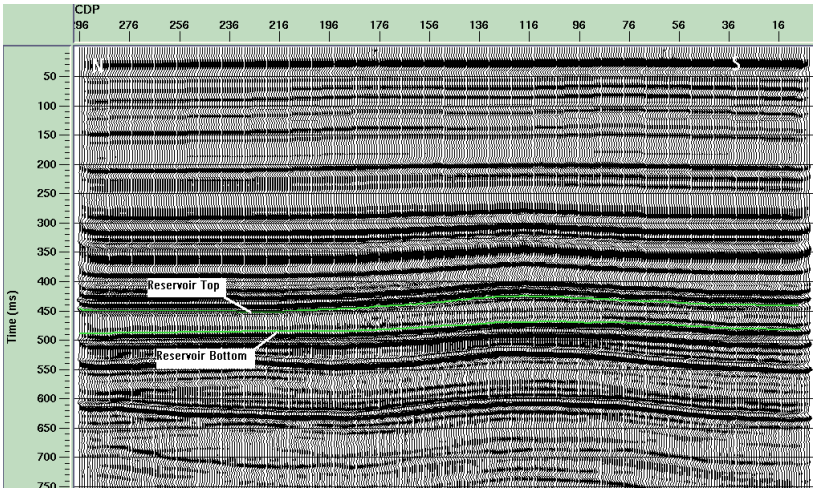

FIG. 9. Synthetic seismic section for Jan. 1981 reservoir condition.

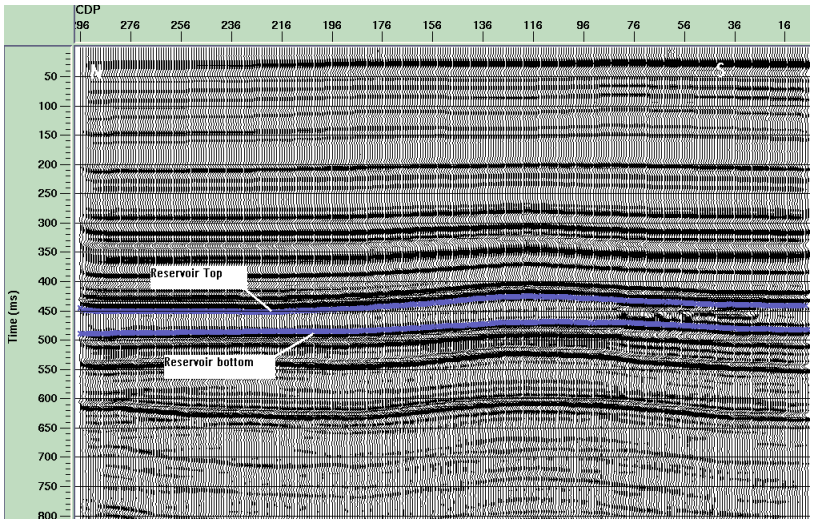

FIG. 10. Synthetic seismic section for Feb. 1991 reservoir condition.

Figure 9, 10 and 11 are the migrated sections corresponding to the time of Jan 1981, Feb 1991 and March 2000, respectively. The synthetic seismic sections are displayed with the same level of whole window gain. The character of the seismic profile changes in the southern part of the reservoir on the 1991 and 2000 sections compared to the 1981 section.

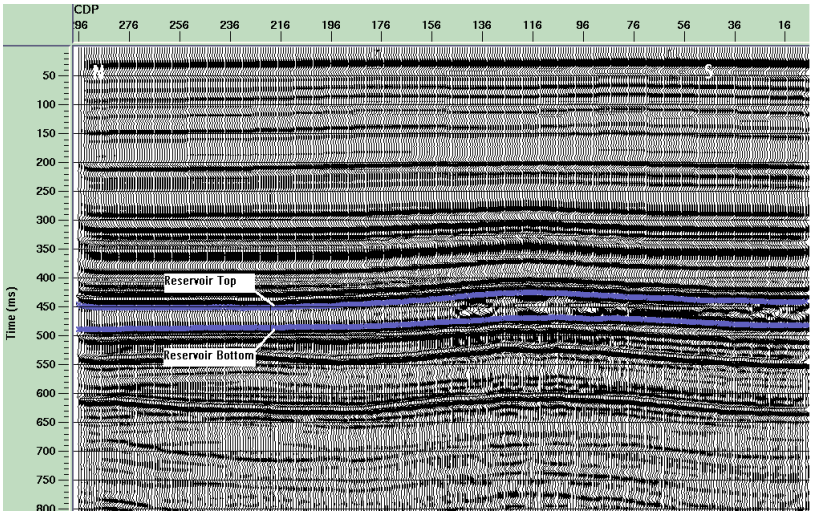

FIG. 11. Synthetic seismic section for March 2000 reservoir condition.

SEISMIC DIFFERENCE ANALYSIS

Difference sections are used to illustrate the relationship between reservoir conditions and seismic changes. Figure 12 is the difference section between the 1991 and 1981 synthetic seismic sections and Figure 13 is the difference section between the 2000 and 1991 synthetic sections. The simulated gas saturation distributions are plotted in Figure 12 (1991) and 13 (2000). Gas saturation in 1981 is zero. On the two difference sections, we observed following phenomena. First, the seismic difference energy appears around areas with active wells. Well 1D2-6 has been in CSS operation since 1983, wells 4A2-6, D2-6 and 4D2-6 since 1993, the T wells started CSS in 1995 and the V wells started CSS in 1997 (Figure 9). In Figure 12, the difference energy is around well 1D2-6 and not in the regions of the other wells. In Figure 13, the difference energy is around the high temperature injection and production areas. Second, difference energy is visible around 600 ms and 750 ms at some CDP locations but is restricted to the top of the reservoir at other CDP locations.

Comparing the saturation, temperature, and pressure results from the reservoir simulation (Figure 5, 6, 7, and 8), we make the following observations:

1) The area with a gas saturation difference between two compared time steps have seismic differences, because the presence of gas reduces the bulk modulus and bulk density of the saturated rock (Domenico, 1974).
2) Thicker gas zones correspond with larger traveltime delays in the seismic section. The thin gas zones only induce large reflectivity, and do not have enough time-delay to be visible in the deeper regions of the seismic section below the reservoir zone.
3) High temperature regions also correlate with areas having seismic energy differences but the correlation is not as strong as the correlation with the gas saturation differences.
4) Pressure spreads very quickly and its value depends on whether the location is in the injection or production stage.

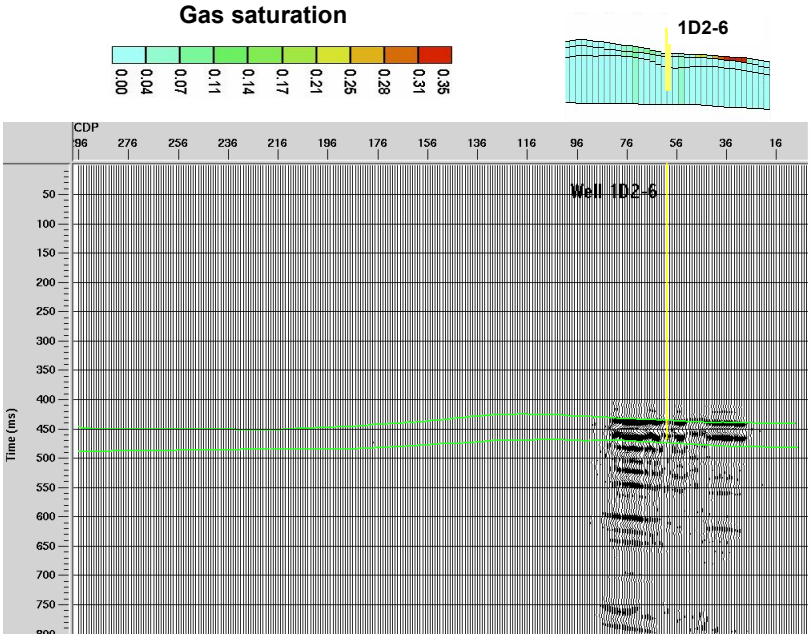

FIG. 12. The difference plot between 1991and 1981 synthetic seismic and gas saturation.

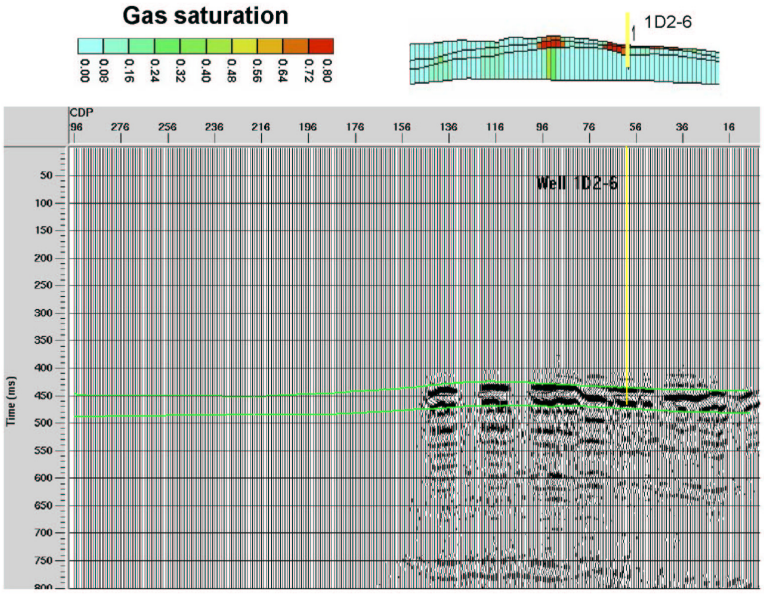

FIG. 13. The difference plot between 2000 and 1991 synthetic seismic and gas saturation.

The pressure dependence of the seismic is not as large as the temperature dependence. The dependence on pressure is due to its influences on gas saturation. However we have not yet accounted for the pressure dependence of the dry bulk moduli. Pressure changes will induce effective pressure changes that cause the dry bulk moduli to change. The pressure induced changes may be significant because the sands are unconsolidated and are at moderate confining stresses. We will consider dry bulk moduli change with effective pressure in future work.

CONCLUSIONS

We have conducted a reservoir simulation based on engineering parameters and production history. The history match is generally good. We also undertook seismic modelling based on our previous procedure and the porosity, temperature, pressure, and fluid saturation distributions from a reservoir simulator. The following results have been obtained:

1) Gas saturation is the dominant factor for high seismic difference energy because the presence of gas reduces the bulk modulus and density of the saturated rock.

2) Thicker gas zones correspond to more time delay in seismic traveltime. We could use this to infer the relative gas zone thickness from relative time delay.

3) High temperature regions correspond to seismic difference energy, but the impact on the seismic response is not as dramatic as gas saturation.

4) Pressure effects to seismic response are minor, but changes to the moduli due to the effective pressure have yet to be incorporated into the rock physics model.

5) The results indicate that the change in seismic response due to 10 years of CSS time can be observed on seismic difference sections.

FUTURE WORK

Procedures for seismic survey analysis, reservoir simulation, and seismic modelling for the Pikes Peak oilfield (Zou, Bentley, and Lines, 2003) have been developed. The moduli dependence on effective stress will be incorporated in the rock physics model. The synthetic seismic sections will be compared with real seismic survey sections. Parameters in the reservoir simulation model will be modified to improve the match between the synthetic and real seismic sections. The objective is to produce a reservoir flow model that can match both production and seismic history. Ultimately, these procedures should improve the understanding of the reservoir and improve the reliability of flow simulations.

ACKNOWLEDGEMENTS

We thank the CREWES sponsors for their support. Special thanks go to Husky Oil for providing the data used in this study and to Larry Mewhort and Don Anderson from Husky for their help with engineering data and their input to this work. We also thank the Computer Modelling Group (CMG) for the use of STARS simulator. We appreciate the help of Dennis Coombe and Peter Ho at CMG during the simulation work.

REFERENCES

Batzle, M. and Wang, Z., 1992, Seismic properties of pore fluids: Geophysics, **57**, No. 11, 1396-1408.

Domenico, S. N., 1974, Effect of water saturation on seismic reflectivity of sand reservoirs encased in shale: Geophysics, **39**, No. 6, 759-770.

Eastwood, J., Lebel, P., Dilay, A., and Blakeslee, S., 1994, Seismic monitoring of steam-based recovery of bitumen: The Leading Edge, **13**, No. 4, 242-251.

Jenkins, S., D., Waite, M., W., and Bee, M., F., 1997, Time-lapse monitoring of the Duri steamflood: A pilot and case study: The Leading Edge, **16**, No. 9, 1267-1273.

Lumley, D. E., 1995, Seismic Time-lapse monitoring of subsurface fluid flow: Ph.D. Thesis, Stanford Exploration Project, Stanford University.

Miller, K. A. and Given, R. M., 1989, Evaluation and application of Pikes Peak cyclic steam injection pressure data: JCPT, **28**, No. 1, 26-32.

Sheppard, G.L., Wong F.Y., and Love D., 1998, Husky's success at the Pikes Peak thermal project: UNITAR Conference, Beijing, China.

Zou, Y. and Bentley, L. R., 2003, Time–lapse well log analysis, fluid substitution, and AVO: The Leading Edge, **22**, No. 6, 550-554

Zou, Y., Bentley, L. R. and Lines, L. R., 2003, Seismic modelling for a heavy oil reservoir time-lapse study: SEG Convention, Dallas